Thermal conductivity measurements of refrigerant mixtures containing hydrofluorocarbons (HFC-32, HFC-125, HFC-134a), hydrofluoroolefins (HFO-1234yf), and carbon dioxide (CO_2)

Dongchan Kim[1], Xiaoxian Yang[1], Arash Arami-Niya[1, 2], Darren Rowland[1], Xiong Xiao[1], Saif Al Ghafri[1], Tomoya Tsuji[3], Yukio Tanaka[4], Yoshio Seiki[4], Eric F. May[1,*]

[1] Fluid Science & Resources Division, Department of Chemical Engineering, University of Western Australia, Crawley, WA 6009, Australia

[2] Discipline of Chemical Engineering, Western Australian School of Mines: Minerals, Energy and Chemical Engineering, Curtin University, GPO Box U1987, Perth, WA 6845, Australia

[3] Malaysia-Japan International Institute of Technology, Universiti Teknologi Malaysia, Kuala Lumpur54100, Malaysia

[4] Chemical No.2 Laboratory, Chemical Research Department, Research & Innovation Center, Mitsubishi Heavy Industries, Ltd., 717-1, Fukahori-machi, 5-chome, Nagasaki, 851-0392, Japan

Abstract

Thermal conductivity measurements of eight binary refrigerant mixtures were conducted in the homogeneous liquid and vapour phases with the transient hot-wire technique. The temperature range of the measurements spanned from (224.3 to 386.6) K with pressures ranging between (1.0 and 6.5) MPa. The binary mixtures were equimolar (R125 + R32), (R32 + R134a), (R32 + CO_2), (R125 + R134a), (R125 + CO_2), (R134a + R1234yf), (R134a + CO_2) and (R1234yf + CO_2). Additionally, two multi-component mixtures, (R32 + R1234yf + CO_2) and (R32 + R1234yf + R134a + R125 + CO_2), were investigated. The transient hot-wire apparatus was validated with measurements of pure CO_2 in the liquid and vapour regions. The relative combined expanded uncertainty (k = 2) in the experimental thermal conductivity was on the order of 2.0 %. The relative deviations of the measured thermal conductivities in the vapour phase from those calculated using the extended corresponding states (ECS) model with default binary interaction parameters (BIPs), as implemented in the software REFPROP 10, were between (–12 and +8) %, while those in the liquid phase were between (–15 and +4) %. The new experimental data were used to tune the BIPs in the ECS model. Significant improvements were observed especially in the liquid phase of the five-component mixture, with the root-mean-square of the relative difference between the experimental data and the model estimation reduced by a factor of nearly three.

Keywords: Thermal conductivity; transient hot-wire; carbon dioxide; hydrofluoroolefins; hydrofluorocarbons

[*]Corresponding author. *Email address:* eric.may@uwa.edu.au.

1. Introduction

To deal with environmental problems, many developed and developing countries are considering more eco-friendly refrigerants with low ozone depletion potential (ODP) and global warming potential (GWP) in the air-conditioning applications[1-2]. After phasing out of the first generations of refrigerants such as chlorofluorocarbons (CFCs) and hydrochlorofluorocarbons (HCFCs), refrigerants with zero ODP including hydrofluorocarbons (HFCs) and hydrofluoroolefins (HFOs) are increasingly being studied and used[3-7]. In particular, recently introduced HFOs offer very low GWP[8-9]. However these environmentally friendly refrigerants suffer from a mild level of flammability. Carbon dioxide (CO_2) as a non-toxic, non-flammable natural refrigerant with comparatively low GWP is a potential candidate for blending with mixtures of HFOs and HFCs to improve the safety of the resulting refrigerant. Mixtures of CO_2, HFOs and HFCs could be used as the next generation of refrigerants, within air-conditioning systems for houses and automobiles.

However, there is a lack of experimental thermophysical property data for refrigerant mixtures containing HFOs, HFCs and CO_2, especially for thermal conductivity. The thermal conductivity of the refrigerant fluid is important in the heat exchanger design because it is central to the calculation of heat transfer coefficients. A more accurate value of the thermal conductivity can help the lower uncertainty of the heat transfer that can be expected and thus optimize (reduce) the size and cost of the equipment needed to ensure a particular temperature is reached. In this work, we present thermal conductivity measurements for binary and multicomponent mixtures of CO_2, HFO-1234yf, HFC-32, HFC-134a and HFC-125. A summary of the selected literature available for mixtures of these refrigerants is listed in Table 1. In this study, the thermal conductivity of eight equimolar binaries of (R32 + R125), (R32 + R134a), (R32 + CO_2), (R125 + R134a), (R125 + CO_2), (R134a + R1234yf), (R134a + CO_2), and (R1234yf + CO_2) and two multi-component mixtures (R32 + R1234yf + CO_2) and (R32 + R125 + R134a + R1234yf + CO_2) were measured. The measurements were conducted with the transient hot-wire (THW) method. The new accurate experimental data were used to tune the binary interaction parameters (BIPs) in the extended corresponding states (ECS) model, as implemented in the software package REFPROP 10[10] from the National Institute of Standards and Technology (NIST).

Table 1. Thermal conductivity data available in the literature for relevant mixtures.

System	T/K	p/MPa	x_1[a]	Author	Year
R32 +R125	283-298	0.10-1.20	0.19-0.82	Tanaka et al[11]	1995
R32 +R125	233-323	2.00-20.00	0.00-1.00	Ro et al[12]	1997
R32 +R125	213-293	2.00-30.00	0.43-0.87	Gao et al[13]	2000
R32 +R125	243-333	0.26-3.90	0.55-0.83	Tomimura et al[14]	2014
R32 +R134a	223-323	2.00-25.00	0.00-1.00	Ro et al[15]	1995
R32 +R134a	254-361	0.08-11.69	0.30-0.70	Perkins et al[16]	1999
R32 +R134a	193-316	2.00-30.00	0.40-0.85	Gao et al[13]	2000
R125 +R134a	244-347	0.07-19.69	0.30-0.70	Perkins et al[16]	1999
R125 +R134a	233-323	2.00-20.00	0.00-1.00	Jeong et al[17]	1999

[a] x_1 is the mole fraction of the first component of the binary mixture in the 'System' column.

2. Experimental

2.1. Measuring principle

The transient hot-wire (THW) method is an absolute method[18-19] from which the thermal conductivity is calculated based on the transient temperature increase of a wire when a step voltage is applied to it. A constant heat flux per unit length, q, is generated along the wire, which produces a temperature rise, ΔT, as a function of time. Assael et al.[20] presented an ideal model for ΔT based on an infinitely-long vertical wire of zero heat capacity and infinite thermal conductivity immersed in the fluid. According to the ideal model, ΔT varies linearly as a function of the logarithm of time, with a slope that depends on the fluid's thermal conductivity. Specifically, the transient temperature increase of the ideal wire is given by

$$\Delta T\,(r_0,\,t) = \frac{q}{4 \cdot \pi \cdot \boldsymbol{\lambda}} \cdot \ln\left(\frac{4\kappa t}{r_0^2 e^{\gamma}}\right) \tag{1}$$

where λ is the fluid's thermal conductivity, t is the measurement time, r_o is the radius of the wire, κ is the fluid's thermal diffusivity, and γ is the Euler constant.

A transient-hot wire apparatus based on the design developed by Perkins et al.[21] was used in this work, as shown in Figure 1. The experimental setup and measurement principle and experimental procedure were explained in detail previously[6, 22]. Although the experimental set-up described for the measurement of the thermal conductivity was designed to approximate the assumptions upon which the ideal model is based, departures from the ideal model need to be considered when analysing any real THW experiment. Suitable experimental design and

measurement conditions are essential for minimizing the departures from the ideal model[23-24]. To account for unavoidable departures from ideality, three main corrections must be applied to adjust the experimental data[22]. These corrections account for: 1) the finite heat capacity of the platinum wire; 2) the finite boundaries associated with the dimensions of the wire and cylindrical pressure vessel; and 3) the effect of radiation. Each correction is generally less than 1% of the experimental temperature increase so that they can be analysed using the ideal model to deliver an accurate determination of the fluid's thermal conductivity. In practice, the contribution of these corrections to the value of the thermal conductivity determined from the data is usually less than 0.1%. The corrections and their application to measurements made with the THW apparatus used in this work are detailed by Mylona et al.[22]

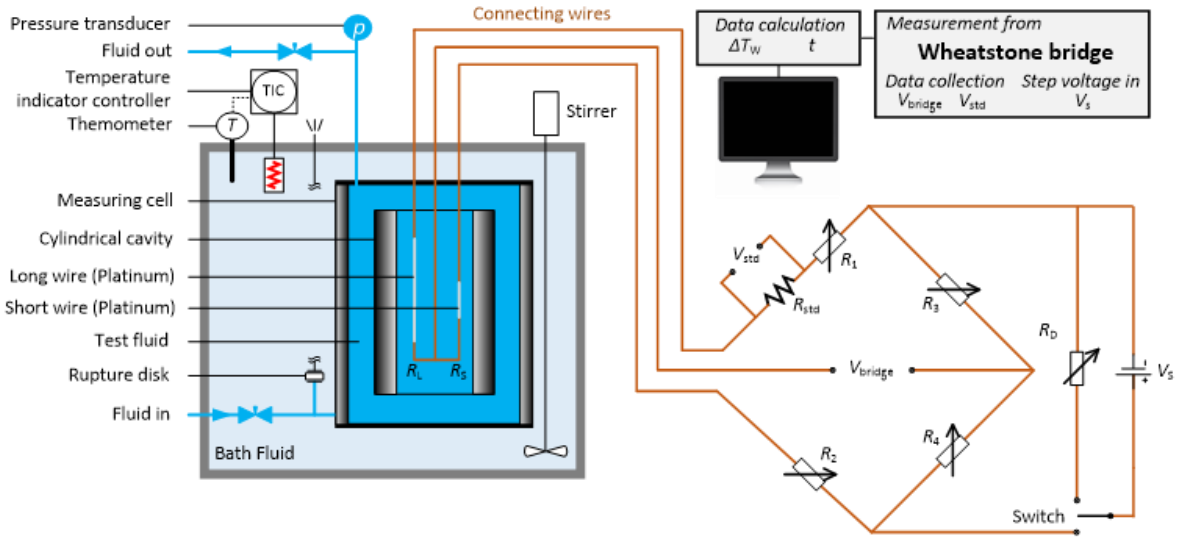

Figure 1. Schematic diagram of the measuring system.

2.2. Measurement procedure

Measurements were conducted with the fluid mixture in the liquid phase first and then in the gas phase. The preparation of the liquid mixture sample and the method by which it was transferred into the THW cell followed the procedure described previously[5-6], and the subsequent procedure for measuring the fluid's thermal conductivity followed the detailed description given by Mylona et al.[22] Here we only present further detail regarding how any vapor-liquid equilibrium condition (which would result in an inadvertent change in liquid composition) was avoided in the process of transitioning the sample from a homogenous liquid to a homogenous gas.

A phase-specific measurement procedure was followed, as depicted in Figure 2 for the measurements of the liquid phase (and in the supercritical region) and in Figure 3 for the measurements of the gas phase. The measurements always commenced with the mixture in the

liquid phase, with the fluid in the measuring cell in contact with the single-phase liquid within the syringe pump was used to control the system pressure (see Figure 2). After the measurements in the liquid phase were complete, the liquid in the measuring cell was pressurized to at least 1 MPa higher than the critical pressure and then heated slowly with a rate less than 0.1 K·min^{-1} to a temperate at least 10 K higher than the critical temperature. When the fluid mixture had stabilized at the conditions of the supercritical state, the measuring cell was isolated from the inlet syringe pump, and then the pressure of the fluid mixture was slowly reduced along an isotherm by slightly opening a needle valve between the measuring cell and an outlet syringe pump, which was filled with a fluid at a pressure kept 0.5 MPa below that of the fluid in the cell (see Figure 3). When the designated cell pressure was reached, the isolating needle valve was closed. The measurements in the gas phase were carried out in a sequence of reducing density, which was achieved by the temperature control and the operation of the needle valve.

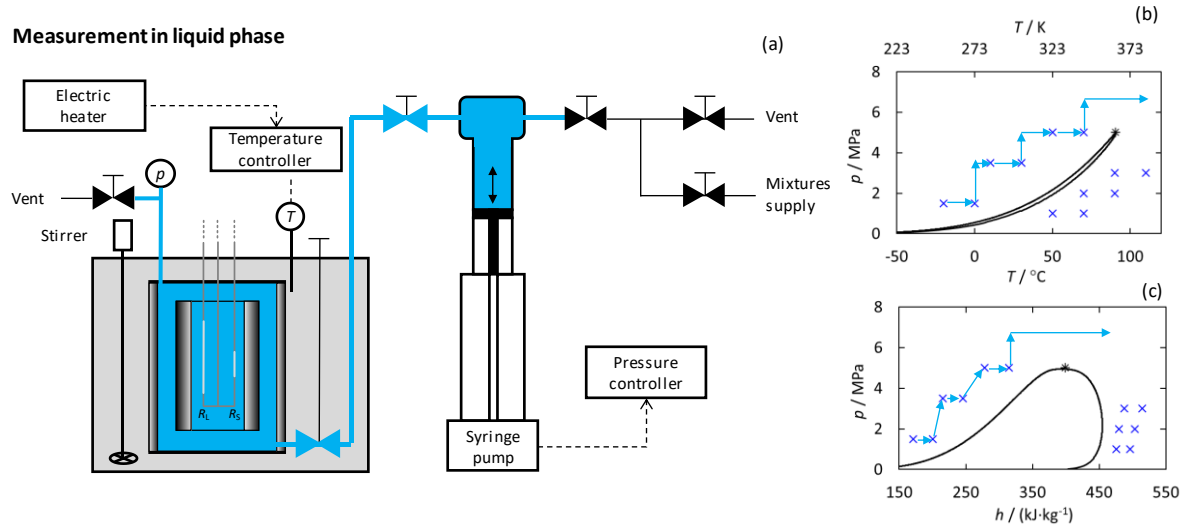

Figure 2. (a) The schematic diagram of the measurements in the liquid phase and in the supercritical region, (b) the pressure-temperature *pT* and (c) pressure-enthalpy *ph* phase diagrams of the exemplar (0.504 R32 + 0.496 R134a) mixture. ×, values measured in the present work; ✳, critical point; –, phase boundaries calculated with REFPROP 10[10]. The arrows denote the steps in the experimental procedure.

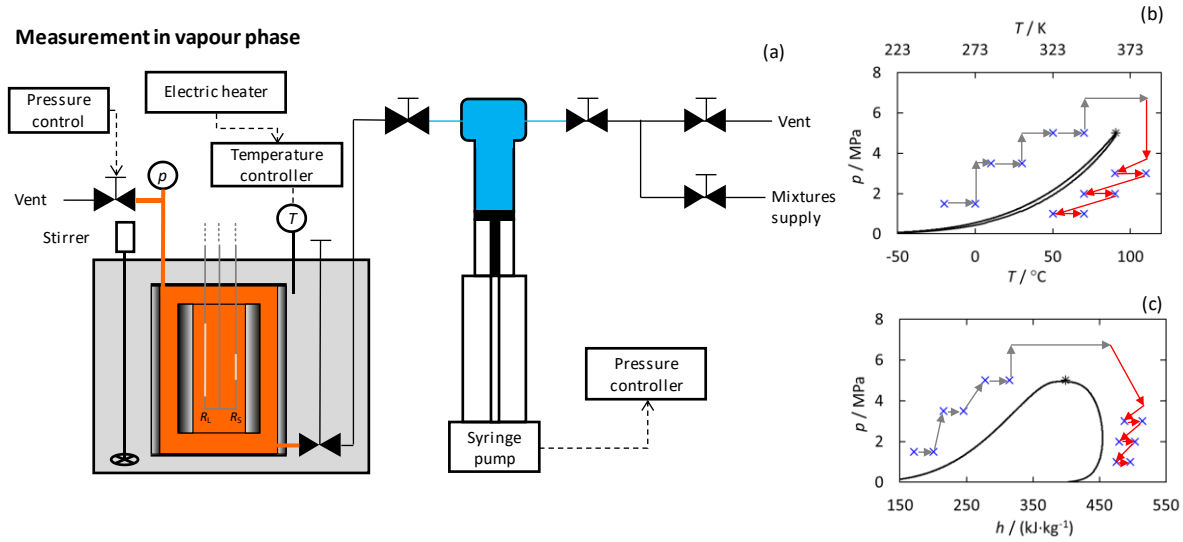

Figure 3. (a) The schematic diagram of the measurements in the gas phase, (b) the pressure-temperature *pT* and (c) pressure-enthalpy *ph* phase diagrams of the exemplar (0.504 R32 + 0.496 R134a) mixture. ×, values measured in the present work; ✳, critical point; –, phase boundaries calculated with REFPROP 10[10]. The arrows denote the steps in the experimental procedure.

2.3. Experimental materials

The pure fluid samples were provided by Coregas, with purities in mole fraction of 0.995 for R32, R125, R134a and R1234yf, and 0.99995 for carbon dioxide. They were used as received from the supplier without further gas analysis or purification. Detailed information for the sample refrigerants is listed in **Table 2**. The binary, ternary and multi-component mixtures were prepared volumetrically in our laboratory using the procedure described by Arami-Niya et al.[3] and Yang et al. [25] with the details of the resulting mixtures listed in

Table **3**.

Table 2. Information for the pure fluid samples

ASHRAE Refrigerant Number	IUPAC name	CAS #	Source	Purity/mole fraction
R32	Difluoromethane	75-10-5	Coregas	0.995[a]
R125	Pentafluoroethane	354-33-6	Coregas	0.995[a]
R134a	1,1,1,2-Tetrafluoroethane	811-97-2	Coregas	0.995[a]
R1234yf	2,3,3,3-Tetrafluoropropene	754-12-1	Coregas	0.995[a]
R744 (CO_2)	Carbon Dioxide	124-38-9	Coregas	0.99995[b]

[a] Purity information was provided by the supplier and no further purification was done.

[b] Impurities (stated by supplier): $x(H_2O) \leq 7\times10^{-6}$, $x(O_2) \leq 1\times10^{-5}$, x(other C_mH_n) $\leq 5\times10^{-6}$, $x(CO) \leq 2\times10^{-6}$, where x denotes mole fraction. No further purification was done.

Table 3. Mole fraction compositions of the mixtures prepared, with expanded ($k = 2$) uncertainties indicated as subscripts in brackets. The numbers in parentheses indicate the uncertainty in the last two digits of the reported mole fraction.

Mixtures	Compositions/mole fraction				
	R32	R125	R134a	R1234yf	R744
Mix. 1	$0.499_{(28)}$	$0.501_{(28)}$	-	-	-
Mix. 2	$0.504_{(28)}$	-	$0.496_{(28)}$	-	-
Mix. 3	$0.499_{(28)}$	-	-	-	$0.501_{(28)}$
Mix. 4	-	$0.500_{(28)}$	$0.500_{(28)}$	-	-
Mix. 5	-	$0.500_{(28)}$	-	-	$0.500_{(28)}$
Mix. 6	-	-	$0.504_{(28)}$	$0.496_{(28)}$	-
Mix. 7	-	-	$0.501_{(28)}$	-	$0.499_{(28)}$
Mix. 8	-	-	-	$0.500_{(28)}$	$0.500_{(28)}$
Mix. 9	$0.434_{(27)}$	-	-	$0.474_{(26)}$	$0.092_{(32)}$
Mix. 10	$0.200_{(22)}$	$0.200_{(22)}$	$0.200_{(23)}$	$0.200_{(16)}$	$0.200_{(29)}$

2.4. Uncertainty analysis

The uncertainty of the measured thermal conductivity was evaluated according to the "Guide to the Expression of Uncertainty in Measurement"[26]. The uncertainties associated with the measured quantities, parameters, calculations, and compositions of the mixture were taken into consideration. A detailed uncertainty analysis was given in our previous work[22]. A budget for the combined uncertainty in the thermal conductivity $U_C(\lambda)$ is listed in

Table **4** with the measurement of the mixture (0.504 R134a + 0.496 R1234yf) at T = 274.50 K and p = 1.04 MPa taken as an example condition. Note that unless otherwise stated, all uncertainties in this work are expanded uncertainties (k = 2) with a confidence level of 95 %. The simplification and corrections applied to the data to enable use of the ideal model, together with the scatter of repeated measurements, are the dominant factors contributing to the overall uncertainty. Across all conditions measured, the value $U_C(\lambda)/\lambda$ was on the order of 2.0 % for all mixtures.

Table 4. Uncertainty budget for the thermal conductivity. The contributions refer to the measurement of (0.504 R134a + 0.496 R1234yf) at T = 274.50 K and p = 1.04 MPa.[a]

Source	Expanded uncertainty U (k = 2)	Contribution to $U_C(\lambda)/\lambda$
Temperature T	100 mK	0.01 %
Voltage on standard resistor V_{std}	0.02 %	0.02 %
Bridge imbalance V_{bridge} (1.5 mV)	0.3 %	0.30 %
Variable resistor R_2	0.05 %	0.03 %
Power supply V_S	0.1 %	0.20 %
Wire radius r (5.0 μm)	0.1 μm	0.03 %
Heat capacity of the wire $c_{p,wire}$	2.0 %	0.03 %
The standard resistor R_{std}	0.1 %	0.10 %
Resistance of the long wire R_L	0.1 %	0.04 %
Resistance of the short wire R_S	0.2 %	0.14 %
Resistance of the working wire R_W	0.3 %	0.30 %
Length of the long wire l_L (0.1515 m)	0.0002 m	0.18 %
Length of the short wire l_S (0.0466 m)	0.0002 m	0.17 %
Regression	10 % of data	0.20 %
Simplification and correction of the ideal model Eq. (1) [b]	1.0 %	1.00 %
Scatter of the repeated measurements	1.1 %	1.10 %
Summary: Combined uncertainty for this mixture $U_C(\lambda)/\lambda$		1.45 %

[a] Uncertainty contributions to $U_C(\lambda)$ associated with pressure measurement p, parameters R_1, R_3, R_4, $R_{L,lead}$, $R_{S,lead}$, α_T, r_{cell}, ρ, c_p and $\rho_{,wire}$, and mixture compositions are less than 0.01 %.
[b] The major simplifications and corrections to the ideal model are those associated with the two-wire technique, the finite heat capacity of the wire, and the boundary confining the fluid to a finite space. See Mylona et al.[22] for futher detail.

2.5. Uncertainty in composition

Al Ghafri et al.[5] described the procedure used to volumetrically prepare and transfer binary refrigerant mixtures into various apparatus, including the THW apparatus used here. In our previous publications[3, 25,] , the formula provided by Al Ghafri et al.[5] for estimating the standard mole fraction uncertainty of each component in the binary was extended to the general case of a multi-component mixture. Since the mixtures prepared in this work were the same as those used by Yang et al.[25] for the viscosity measurements, the uncertainty in mixture composition listed in

Table **3** is as reported previously. These composition uncertainties were combined with sensitivity factors calculated with the ECS model implemented in REFPROP 10.0[10] to estimate the contribution of the composition uncertainties to the combined uncertainty in the measured thermal conductivity.

3. Results and Discussion

3.1. Validation tests

To test the experimental apparatus, thermal conductivity measurements of carbon dioxide were carried out in the temperature range from (234.3 to 397.9) K and at pressures between (0.4 and 8.1) MPa, conditions which include the vapour and liquid phases. Carbon dioxide was chosen because it is a major component of the investigated mixtures. The experimental temperature increase of the wire ΔT as a function of time t, and the relative deviations of the data from the fit to Eq. (1) are shown in Figure 4 for the exemplar measurement of at T = 393.15 K and p = 2.00 MPa. The measured ΔT values deviate by less than 0.05 % from the linear fit to ln(t), indicating operation of the THW sensor during the carbon dioxide measurements was appropriate for analysis with Eq. (1).

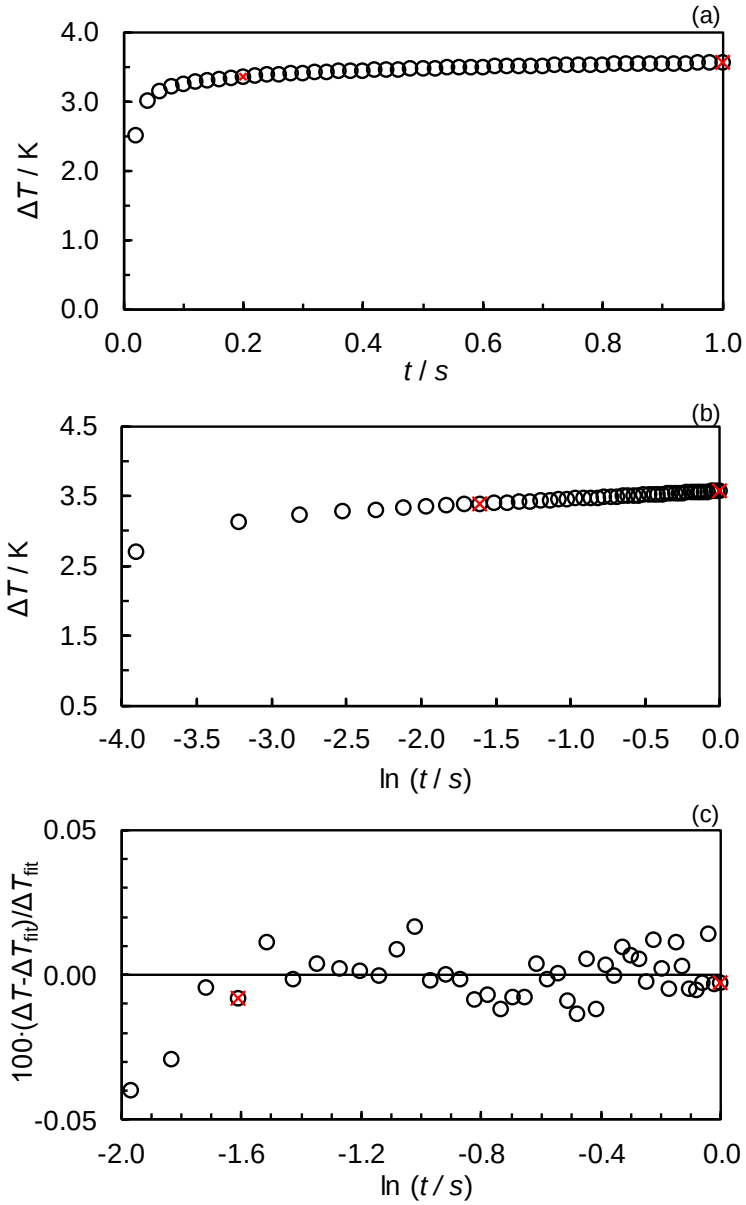

Figure 4. The experimental temperature increase of the wire ΔT as a function of time t (a), and $\ln(t)$ (b), respectively, for the carbon dioxide measurement at T = 393.15 K and p = 2.00 MPa. (c) Relative deviations of ΔT values from the fit ΔT_{fit} to Eq. (1). ○, measured points; × indicating the start and end times used for the fit.

Carbon dioxide absorbs infrared radiation, which influences the transfer of heat through the fluid significantly in comparison with other fluids. To account for this effect, a radiation correction was applied to the raw temperature rise data following the method of Perkins et al.[21]. Specifically, equation (9) of Perkins et al.[21] was used for the radiation correction and equations (12) and (13) of Perkins et al.[21] were used to estimate the associated radiation parameter. The radiation effect is particularly significant for the gas phase in the vicinity of the critical point. To demonstrate this, two different measurement conditions at (313.15 K, 4.05 MPa) and (393.15 K, 3.03 MPa) were investigated with the former one near the critical point. The relative deviations of the temperature increase of the wire ΔT before and after the radiation correction from the fit ΔT_{fit} to Eq. (1) as a function of time $\ln(t)$ are illustrated in Figure 5. A significant

improvement in the fitting is achieved when the radiation correction is applied at the measurement condition near the critical point, while no obvious improvement is observed at the other condition.

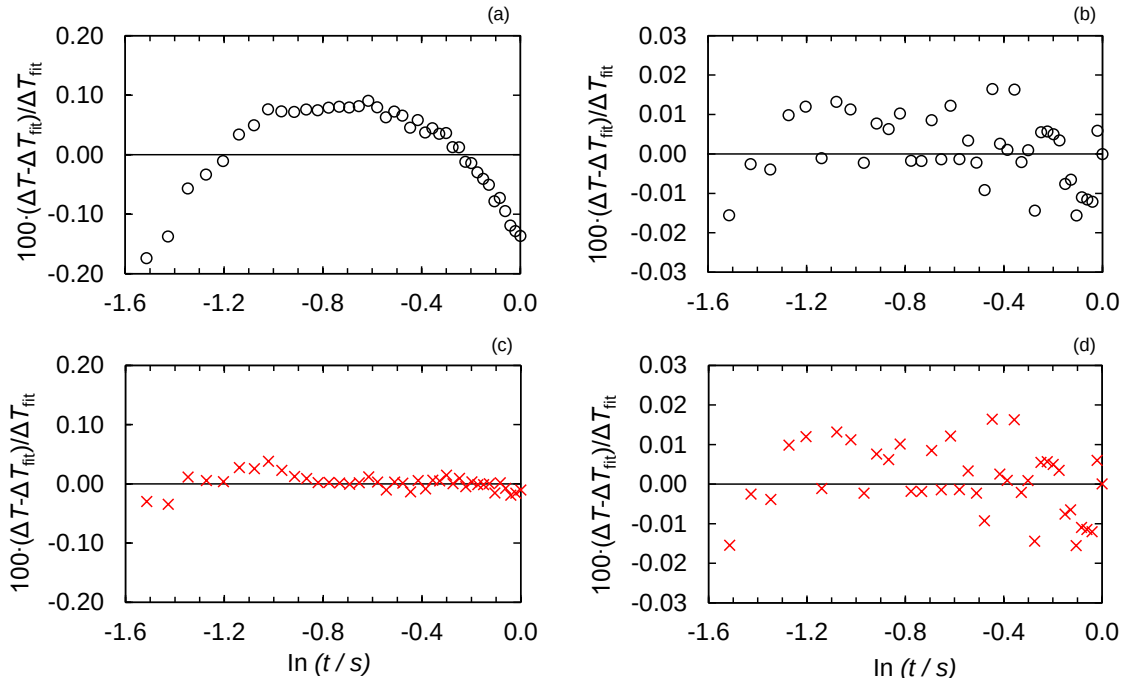

Figure 5. Relative deviations of ΔT values from the fit to Eq. (1), ΔT_{fit}, as a function of time ln(t) for two CO_2 measurements. Measurement condition at T = 313.15 K and p = 4.05 MPa, (a) without and (c) with the radiation correction. Measurement condition at T = 393.15 K and p = 3.03 MPa, (b) without and (d) with the radiation correction. ○, no radiation correction applied; ×, radiation correction applied.

The corrected results are summarized in Table 5, while Figure 6 shows the conditions of the CO_2 measurements together with the relative deviations of the thermal conductivity data from corresponding values predicted with the reference equation[27] implemented in REFPROP[10]. The relative magnitude of the radiation correction was largest for the gas phase particularly at temperatures near the critical point: at 304.55 K the radiation correction of –2.2 mW·m^{-1}·K^{-1} amounted to –9.7 % of the thermal conductivity at that temperature. At liquid phase conditions, the correction was larger in absolute terms but smaller on a relative basis. Application of the radiation correction reduced the average relative deviation from 2.9 % to –0.2 %; however the scatter of the deviations from the model increased in the gas phase to around ± 5.0 %. This likely reflects the difficulty of accurately correlating the appreciable critical enhancement of thermal conductivity in a pure fluid, even at densities far removed from critical density.

Table 5. The thermal conductivity of carbon dioxide measured in this work.[a]

T **/K**	***p*** **/MPa**	λ_{exp} **/(W·m^{-1}K^{-1})**	***T*** **/K**	***p*** **/MPa**	λ_{exp} **/(W·m^{-1}K^{-1})**
liquid phase					

234.32	4.984	0.1642	254.42	6.530	0.1410
234.33	6.546	0.1664	254.19	8.036	0.1461
234.22	8.056	0.1684	274.36	5.015	0.1110
254.28	5.064	0.1398	274.44	6.536	0.1176
			274.21	8.069	0.1205
		gas phase			
305.60	0.444	0.0170	355.49	2.952	0.0224
304.55	3.998	0.0200	355.45	3.993	0.0228
315.68	0.972	0.0179	355.38	4.992	0.0245
315.66	2.040	0.0187	365.82	2.047	0.0235
315.25	3.017	0.0193	375.29	0.367	0.0238
315.41	4.001	0.0201	375.45	0.577	0.0226
314.47	5.000	0.0223	375.50	0.773	0.0223
325.29	0.416	0.0185	376.25	1.981	0.0238
336.15	0.971	0.0196	375.03	3.001	0.0233
335.81	2.008	0.0202	375.42	3.988	0.0243
335.45	2.952	0.0206	375.09	5.013	0.0245
335.10	3.974	0.0217	385.43	4.045	0.0269
335.08	4.990	0.0224	397.92	0.984	0.0262
344.96	3.999	0.0227	396.79	1.995	0.0266
355.45	0.427	0.0219	396.30	2.981	0.0263
356.04	0.950	0.0218	396.28	3.991	0.0268
355.85	1.978	0.0222	395.96	5.003	0.0275

[a] The expanded uncertainties ($k = 2$) of the measurements are 0.10 K for temperature T, 0.040 MPa for pressure p, and in the order of 2.0 % for thermal conductivity λ.

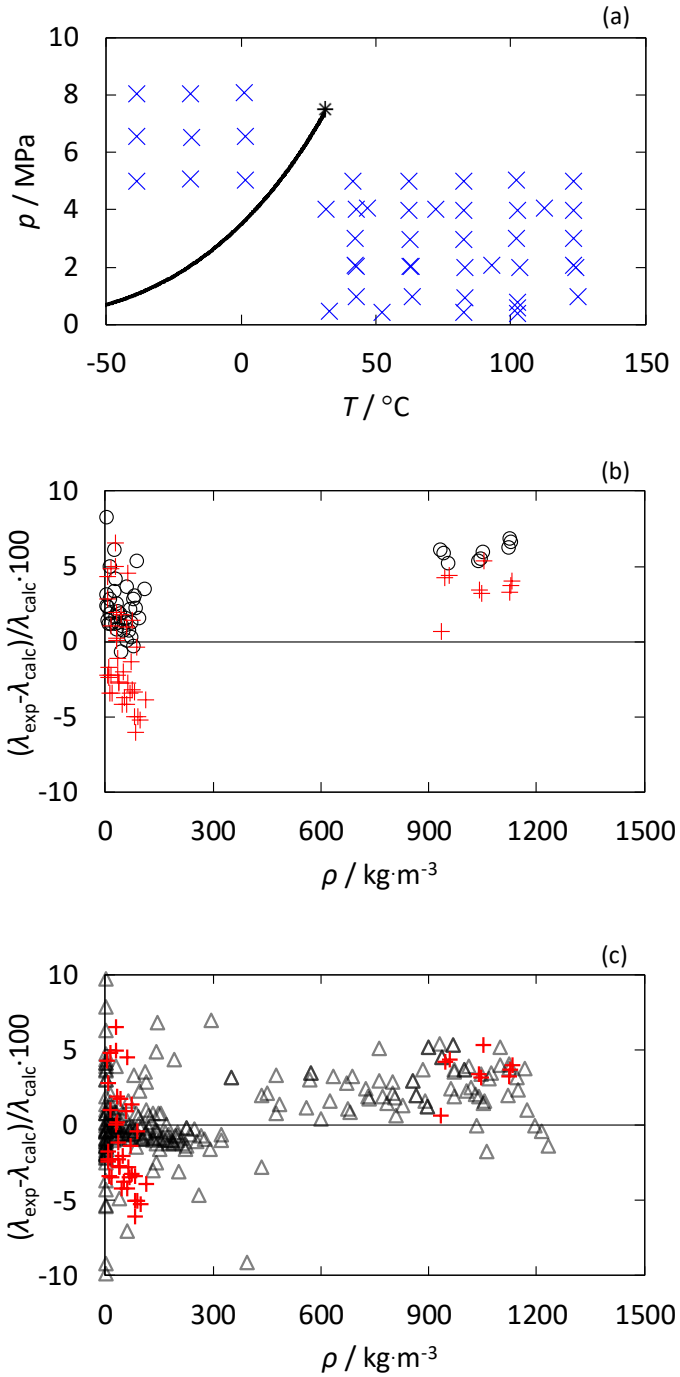

Figure 6. (a) The pressure-temperature *pT* phase diagram of CO_2. The phase boundaries (solid curve) together with the critical point (✳) were obtained from REFPROP 10[10] and '×' denotes the points measured in this work work. (b) The relative deviations of the experimental thermal conductivites λ_{exp} from those calculated λ_{calc} using the ECS model[28] implemented in REFPROP 10[10]. ○, data of this work without radiation correction; +, data of this work with radiation correction. (c) Relative deviations of the data measured in this work with the radiation correction applied, and for the data, △, obtained from the NIST TDE database[27] from those calculated using the ECS model.

Since all the refrigerants investigated absorb infrared radiation[21, 29], the radiation correction was applied to all the refrigerant mixtures investigated. While the magnitude of the radiation correction is fluid and temperature specific, it can be estimated directly from the temperature

rise data measured for that fluid at a given condition; as demonstrated by Perkins et al.[21] no prior knowledge of the fluid's optical properties is required to estimate or apply the radiation correction. The radiation correction method proposed by Perkins et al.[21] was able to roughly estimate the radiation effect from the raw temperature rise data and it was found that the radiation effect could not be ignored for any of the mixtures investigated, producing a relative change in thermal conductivity on the order of 3.0 %. We recommend routinely evaluating the radiation correction by Perkins et al.[21] for fluids likely to absorb infrared radiation to determine whether the radiation effect should be corrected.

3.2. Measurement results

The results of the thermal conductivity measurements for the binary, ternary and five-component refrigerant mixtures are presented in Table 6. A few experiments were conducted twice to check the repeatability of the measurements. The density of the fluid mixture, ρ_{EOS}, is needed to calculate the fluid's thermal diffusivity κ and to evaluate the corrections associated with the finite heat capacity of the wire[22] to the ideal model shown in Eq. (1). At each temperature and pressure ρ_{EOS} was calculated using the mixture's Helmholtz equation of state (EOS) implemented in the REFPROP 10.0[10]. The default binary parameters in the Helmholtz EOS for these mixtures were, however, not used. Instead, the optimized binary parameters determined by Arami-Niya et al.[3] after tuning to the density, VLE and heat capacity data they measured for these same mixtures were used to make the mixture density estimate more accurate. Nevertheless, the impact of the improved density predictions on the measured thermal conductivity, λ_{exp}, is small. For example, at T = 254.36 K and p = 3.47 MPa of the mixture (0.500 R1234yf + 0.500 CO_2), the predicted density value changes by as much as 1.3 % if the optimized binary parameters by Arami-Niya et al.[3] are used instead of the default ones, while the resulting change in the value of λ_{exp} is less than 0.01 %. All the mixture density values estimated in this work were calculated with the optimized binary parameters determined by Arami-Niya et al.[3], unless otherwise stated.

Table 6. Thermal conductivity λ_{exp} data measured for the mixtures together with the combined, expanded uncertainty ($k = 2$) $U_C(\lambda)$[a] and mixture density, ρ_{EOS}.[b]

T /K	p /MPa	ρ_{EOS} /(kg·m^{-3})	λ_{exp} /(W·m^{-1}K^{-1})	$U_C(\lambda)$ /(W·m^{-1}K^{-1})	T /K	p /MPa	ρ_{EOS} /(kg·m^{-3})	λ_{exp} /(W·m^{-1}K^{-1})	$U_C(\lambda)$ /(W·m^{-1}K^{-1})
Vapour Phase					Liquid Phase				
0.499 R32 + 0.501 R125[c]									
304.30	1.03	40.83	0.01532	0.00019	254.25	1.51	1305.86	0.0990	0.0013
325.50	1.04	37.09	0.01689	0.00022	274.20	1.51	1225.57	0.0882	0.0012
324.71	2.05	85.85	0.01810	0.00030	274.15	3.51	1237.49	0.0899	0.0011
345.04	2.00	72.70	0.02004	0.00027	303.80	3.52	1096.72	0.0754	0.0011
345.59	3.03	127.08	0.02181	0.00035	303.88	5.05	1112.94	0.0767	0.0009
366.36	3.01	108.06	0.02233	0.00035	323.44	5.01	994.01	0.0695	0.0010
0.504 R32 + 0.496 R134a									
325.31	1.06	34.80	0.01653	0.00024	254.46	1.50	1264.42	0.1202	0.0014
345.20	0.98	29.07	0.01741	0.00022	274.35	1.50	1199.29	0.1089	0.0016
345.33	2.09	72.27	0.02091	0.00030	284.42	3.52	1172.62	0.1048	0.0013
364.73	2.04	62.41	0.02050	0.00026	305.48	3.48	1092.33	0.0906	0.0011
365.65	2.86	96.59	0.02055	0.00025	323.95	5.00	1022.22	0.0805	0.0010
385.13	3.06	93.37	0.02250	0.00032	333.69	5.00	971.95	0.0748	0.0009
0.499 R32 + 0.501 CO_2									
284.60	1.13	25.76	0.01344	0.00063	224.38	1.66	1184.85	0.1791	0.0023
314.31	1.15	22.88	0.01556	0.00069	244.40	1.60	1117.46	0.1605	0.0021
314.24	2.64	59.97	0.01740	0.00064	244.53	3.58	1122.55	0.1628	0.0019
334.35	2.64	53.49	0.01840	0.00065	274.47	3.48	1005.98	0.1322	0.0016
354.00	5.14	111.11	0.02332	0.00067	274.11	5.07	1015.46	0.1346	0.0016
358.37	6.53	151.84	0.02534	0.00069	294.14	5.10	918.60	0.1109	0.0014
0.500 R125 + 0.500 R134a									
324.65	1.07	52.07	0.01625	0.00037	255.28	1.01	1383.45	0.0887	0.0011
344.79	1.04	45.58	0.01903	0.00038	274.58	1.01	1311.43	0.0804	0.0010
355.52	2.07	100.29	0.01903	0.00038	274.52	2.03	1317.16	0.0814	0.0012
375.85	2.03	86.94	0.02078	0.00040	304.26	2.03	1188.00	0.0664	0.0008
376.76	3.08	150.63	0.02449	0.00046	304.31	2.99	1197.14	0.0685	0.0009
386.64	3.70	182.98	0.02340	0.00044	323.38	3.00	1093.24	0.0632	0.0008
0.500 R125 + 0.500 CO_2									
304.58	1.02	36.37	0.01598	0.00020	234.11	2.07	1359.67	0.1014	0.0012
314.84	1.01	34.40	0.01682	0.00021	254.14	2.00	1273.33	0.0892	0.0011
314.47	2.04	77.59	0.01768	0.00021	254.22	3.56	1281.21	0.0915	0.0012
334.33	2.04	69.67	0.01994	0.00025	274.17	3.55	1183.60	0.0775	0.0011
334.42	3.99	168.17	0.02219	0.00030	274.35	5.02	1194.35	0.0778	0.0010
354.59	4.03	145.23	0.02304	0.00029	298.98	5.02	1042.87	0.0643	0.0008
0.504 R134a + 0.496 R1234yf									
335.18	0.98	44.59	0.01835	0.00024	254.86	1.01	1285.99	0.0911	0.0011
354.05	0.96	39.83	0.01801	0.00024	274.50	1.04	1224.44	0.0810	0.0010
354.66	1.46	65.56	0.01851	0.00024	274.41	2.04	1229.15	0.0807	0.0010
365.11	2.05	96.34	0.01933	0.00033	304.30	1.96	1122.66	0.0669	0.0008
375.54	2.50	118.63	0.02208	0.00028	304.28	3.03	1130.53	0.0677	0.0009

385.06	2.99	143.88	0.02262	0.00034	324.40	3.04	1046.34	0.0580	0.0007
0.501 R134a + 0.499 CO_2									
325.17	1.54	47.94	0.01835	0.00022	233.40	1.95	1308.10	0.1267	0.0018
344.85	1.53	43.50	0.02033	0.00026	253.40	2.11	1238.89	0.1126	0.0013
344.81	3.04	100.01	0.02019	0.00025	253.39	3.49	1243.73	0.1134	0.0016
365.01	3.03	88.35	0.02332	0.00031	273.67	3.51	1166.46	0.0983	0.0013
364.72	5.03	178.02	0.02591	0.00033	273.81	4.97	1172.96	0.0972	0.0014
374.46	6.00	214.94	0.02957	0.00040	304.34	5.01	1033.40	0.0833	0.0010
0.500 R1234yf + 0.500 CO_2									
315.02	1.04	34.75	0.01667	0.00020	234.12	2.16	1224.64	0.1024	0.0012
335.13	1.04	31.96	0.01860	0.00025	254.24	2.18	1157.94	0.0921	0.0012
334.68	2.04	69.22	0.01891	0.00025	254.36	3.47	1162.57	0.0933	0.0011
355.08	1.98	60.52	0.02081	0.00027	274.53	3.48	1089.57	0.0742	0.0009
364.81	3.89	133.46	0.02291	0.00028	274.48	4.99	1097.80	0.0759	0.0009
384.43	5.58	193.93	0.02740	0.00032	299.33	5.03	996.31	0.0680	0.0009
0.434 R32 + 0.474 R1234yf + 0.092 CO_2									
314.69	1.05	37.64	0.01568	0.00020	254.62	1.49	1170.59	0.1005	0.0012
335.15	1.06	34.48	0.01736	0.00024	274.49	1.49	1102.62	0.0904	0.0012
344.43	1.90	65.91	0.01952	0.00024	284.36	3.03	1074.39	0.0864	0.0011
354.35	3.06	118.48	0.02438	0.00031	304.10	3.01	991.97	0.0716	0.0010
365.42	1.99	62.48	0.02120	0.00028	314.06	4.51	959.85	0.0699	0.0008
373.94	3.00	99.93	0.02169	0.00028	334.26	4.53	840.39	0.0671	0.0008
0.200 R32 + 0.200 R125 + 0.200 R134a + 0.200 R1234yf + 0.200 CO_2									
315.01	1.04	39.16	0.01589	0.00021	253.94	2.04	1262.33	0.0962	0.0012
335.26	1.04	35.69	0.01778	0.00023	274.30	2.02	1185.78	0.0843	0.0011
344.62	2.08	77.11	0.01954	0.00025	274.17	2.08	1186.63	0.0864	0.0013
354.53	2.98	116.73	0.02159	0.00026	304.22	3.51	1060.98	0.0698	0.0009
365.09	2.02	66.96	0.02124	0.00028	304.32	5.02	1075.52	0.0729	0.0009
375.03	3.05	105.54	0.02316	0.00035	324.12	5.03	965.23	0.0617	0.0008

[a] The expanded uncertainties ($k = 2$) of the measurements are 0.10 K for temperature T and 0.04 MPa for pressure p, while those for the mixture compositions are summarized in

Table 3. [b] ρ_{EOS} is the density calculated with the Helmholtz equations of state for these mixtures implemented in the REFPROP 10.0[10] with binary parameters reported by Arami-Niya et al[3]. [c] The number in front of a component indicates the mole fraction.

Measurements were completed over the temperature range (224.4 to 386.6) K and the pressure range (1.0 to 6.5) MPa. Overall, a total of 120 values of thermal conductivity for ten mixtures were acquired in the range from (0.013 to 0.030) $W \cdot m^{-1} \cdot K^{-1}$ at densities from (23 to 215) $kg \cdot m^{-3}$ for the vapour phase and in the range from (0.058 and 0.179) $W \cdot m^{-1} \cdot K^{-1}$ at densities from (840 to 1383) $kg \cdot m^{-3}$ for the liquid phase, as shown Figure 7 (a) and (b), respectively.

The relative deviations of the measured thermal conductivities in the vapour phase from those calculated using the ECS model with default binary interaction parameters (BIPs) for thermal conductivity were between (–12 and +8) %, while those for the liquid phase were between (–15 to +4) %, as shown in Figure 7 (c) and (d).

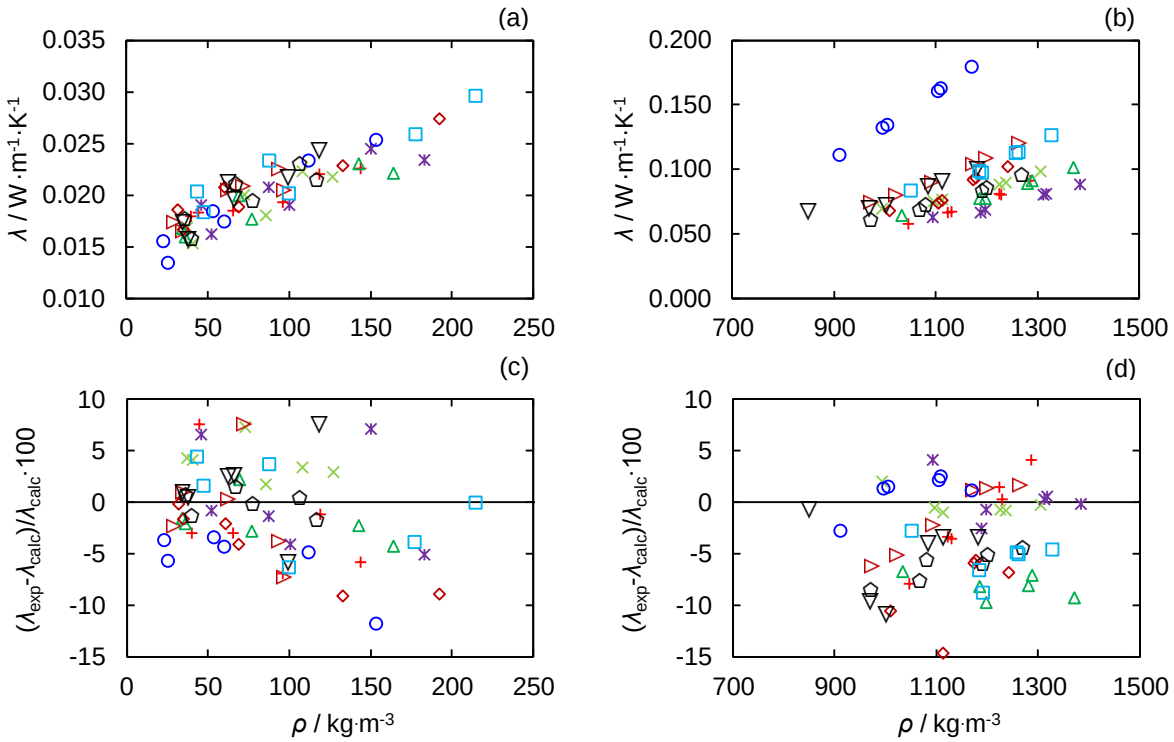

Figure 7. Dependence of the thermal conductivities λ_{exp} measured for the refrigerant mixtures in the (a) vapor phase and (b) liquid phase on density, ρ, and relative deviations of these experimental thermal conductivities from values calculated λ_{calc} with the default ECS model[28] as implemented in REFPROP 10,[10] in the (c) vapor phase and (d) liquid phase . Symbols: ×, R32 + R125; ▷, R32 + R134a; ✱, R125 + R134a; +, R134a + R1234yf; ○, R32 + CO_2; △, R125 + CO_2; □, R134a + CO_2 ; ◇, R1234yf + CO_2; ▽ , R32 + R1234yf + CO_2; ⬠ , R32 + R125 + R134a + R1234yf + CO_2.

In addition, the thermal conductivities measured for (R32 + R125), (R32 + R134a) and (R125 + R134a) were compared with data from the literature summarized in Table 1. These comparisons are shown in Figure 8 in terms of the relative deviations of the data from thermal

conductivities calculated with the ECS model[28] using the default thermal conductivity BIPs in REFPROP 10[10]. Our measurements are generally within the scatter of the literature data except for some points in the gas phase.

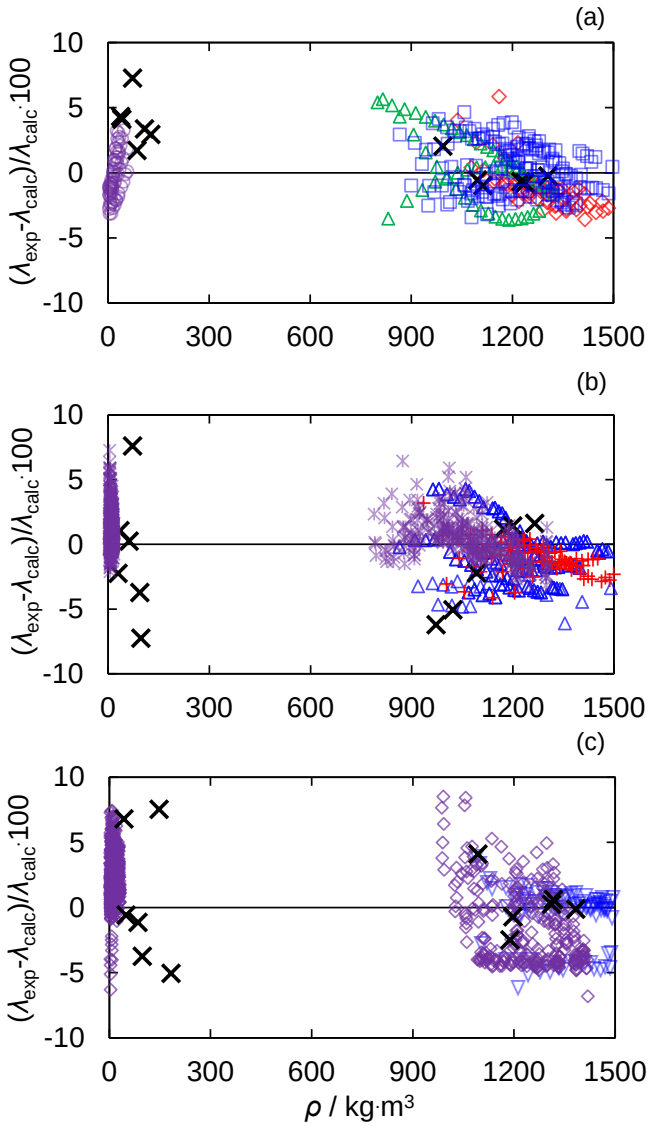

Figure 8. Relative deviations of the experimental thermal conductivity λ_{exp} data from values λ_{calc} calculated with the ECS model[28] using the default thermal conductivity BIPs as implemented in REFPROP 10[10]. (a) R32 + R125: ×, this work; ○, Tanaka et al.[11]; □, Ro et al.[12]; ◇, Gao et al.[13]; △, Tomimura et al.[14] (b) R32 + R134a: ×, this work; +, Gao et al.[13]; △, Ro et al.[15]; ∗, Perkins et al.[16] (c) R125 + R134a: ×, this work; ◇, Perkins et al.[16]; ▽, Jeong et al.[17].

3.3. Tuning the Extended Corresponding States (ECS) model

The ECS model for the thermal conductivity of fluids was developed by Chichester and Huber[30]. It is based on the work of Ely and Hanley[31-32] who developed a procedure that considers the contributions of the transitional and internal modes of molecular motion to the transfer of energy through the fluid. The model for a mixture is based on the model for each

pure component and a mixing rule for each pair of components. Three thermal conductivity BIPs, $k_{ij,\lambda}$, $k_{ij,f\lambda}$ and $k_{ij,h\lambda}$ were modified when experimental data for the binary system were available; otherwise they were set to zero. In this work, data for eight equimolar binary mixtures were acquired, but only the BIPs for the four binaries containing CO_2 were tuned to the new experimental data. To accurately calculate the thermal conductivity of the multi-component mixtures studied, BIPs for constituent binaries without CO_2 are also needed. Most of these were obtained from the tuning done in our previous work[6], except for the R32 + R1234yf BIPs. No experimental data of R32 + R1234yf are available, and therefore the BIPs for the R32 + R1234yf system were estimated by tuning the ECS model's predictions for the multi-component mixtures to the experimental data measured here for these two systems, as summarised in Table 7.

No tuning was necessary for the remaining three binaries because the predictions of the ECS model with default thermal conductivity BIPs agreed sufficiently well with the experimental data (see Figure 7). The tuning was implemented by changing the BIPs listed in the HMX.BNC file contained within the installed REFPROP[10] software package. A least-squares regression method was used to yield the lowest root-mean-square (RMS) value for the differences between the experimental thermal conductivity and those values calculated with the ECS model.[28]

Table 7. The tuned thermal conductivity binary interaction parameters of the ECS model for the four binary mixtures containing CO_2 considered in this work as well as R32 + R1234yf. These parameters should be used with the binary interaction parameters determined by Arami-Niya et al. for the mixture EOS[3].

System [a]	$k_{ij,\lambda}$	$k_{ij,f\lambda}$	$k_{ij,h\lambda}$
R32 + CO_2	-0.12	0	0.010
R125 + CO_2	-0.030	0	0.140
R134a + CO_2	0.015	0	0.050
R1234yf + CO_2	-0.090	0	0.125
R32 + R1234yf	0.12	0	0.165

[a] Parameters for the four binaries containing CO_2 were tuned to the new experimental data and those for (R32 + R1234yf) were tuned to reduce the deviations in the ternary and five component mixtures.

The RMS values of the differences between the experimental thermal conductivity and values calculated with the ECS model using both the default and tuned thermal conductivity BIPs are summarized in Table 8. Significant improvements were obtained for the four binaries containing CO_2, as shown in Figure 9. Overall, the relative deviations were decreased from a range of (−12 to 5) % obtained with the default thermal conductivity BIPs to (−8 to 5) % with the tuned thermal conductivity BIPs. The thermal conductivity predictions were most obviously improved in the liquid phase of (R125 + CO_2), (R134a + CO_2) and (R1234yf + CO_2), and in the vapour phase of (R32 + CO_2). Furthermore, although the thermal

conductivity predictions for the five-component mixture did not change much in the vapour phase, the RMS deviation for the liquid phase data was reduced by a factor of nearly three.

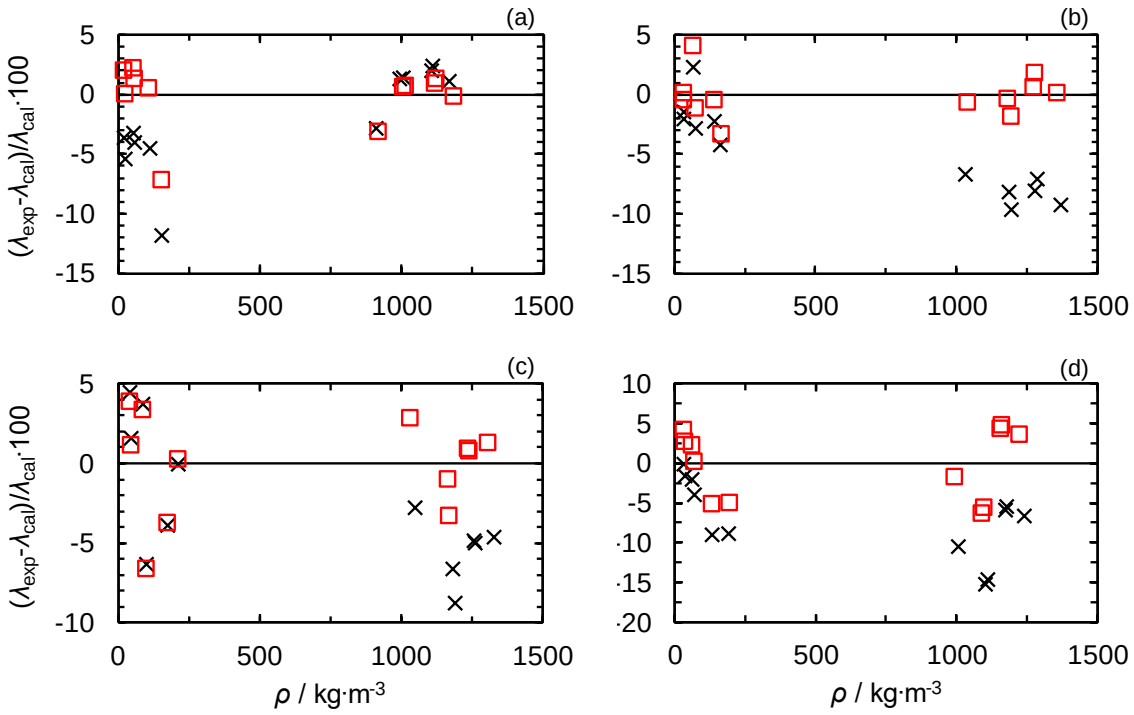

Figure 9. Relative deviations of the thermal conductivities measured for (a) R32 + CO_2, (b) R125 + CO_2, (c) R134a + CO_2 and (d) R1234yf + CO_2 from values calculated with the ECS model with the default parameters (×) and the tuned parameters (□).

Table 8. Summary of the thermal conductivity deviations for the tuned and default ECS models.

System	*N*(vap)	RMS/% (default)	RMS/% (tuned)	*N*(liq)	RMS/% (default)	RMS/% (tuned)
R32 + CO_2	6	6.34	3.13	6	1.98	1.48
R125 + CO_2	6	2.71	2.25	6	8.26	1.12
R134a + CO_2	6	3.91	3.81	6	5.76	1.95
R1234yf + CO_2	6	5.56	3.73	6	10.58	4.63
R32 + R125	6	4.37		6	1.02	
R32 + R134a	6	4.65		6	3.55	
R125 + R134a	6	4.80		6	1.98	
R134a + R1234yf	6	5.15		6	4.18	
R32 + R1234yf + CO_2	6	4.18	4.30	6	6.47	6.25
R32 + R125 + R134a + R1234yf + CO_2	6	2.38	2.47	6	11.70	4.01

4. Conclusions

Thermal conductivity measurements of eight equimolar binary mixtures and two multi-component mixtures of R32, R125, R134a, R1234yf, and CO_2 were investigated in the homogeneous liquid and vapour phases with the transient hot-wire technique in the temperature range from (224.3 to 386.6) K at pressures up to 6.5 MPa. Measurements of pure carbon

dioxide were conducted in both liquid and vapour phases to validate the experimental apparatus and method. The relative combined expanded uncertainty ($k = 2$) in the experimental thermal conductivity was in the order of 2.0 %. The relative deviations of the measured thermal conductivities in the vapour phase from values calculated with the default ECS model in the software REFPROP 10 were between (–12 and +8) %, while those in the liquid phase were from (–15 to +4) %. For binaries of (R32 + R125), (R32 + R134a) and (R125 + R134a), the experimental values of this work are generally within the scatter of the best-selected literature data, except for some data measured in the vicinity of the critical point. The new experimental data for the binaries containing CO_2 were used to tune the thermal conductivity BIPs in the ECS model. This significantly improved the ECS model predictions, particularly in the liquid phase. For the five-component mixture the root-mean-square value of the relative difference between the experimental data and the model predictions for the liquid phase was reduced by a factor of three.

Acknowledgments

This work was supported by Mitsubishi Heavy Industries, Ltd and the Australian Research Council through IC150100019.

References

1. Calm, J. M., The next generation of refrigerants–Historical review, considerations, and outlook. *Int. J. Refrig.* **2008,** *31* (7), 1123-1133.
2. Abas, N.; Kalair, A. R.; Khan, N.; Haider, A.; Saleem, Z.; Saleem, M. S., Natural and synthetic refrigerants, global warming: A review. *Renewable and Sustainable Energy Reviews* **2018,** *90*, 557-569.
3. Arami-Niya, A. X., X.; Ghafri, S. A.; Jiao, F.; Khamphasith, M.; Pouya, E. S.; Seyyedsadaghiani, M.; Yang, X.; Tsuji, T.; Tanaka, Y.; Seiki, Y.; May, E. F., Measurement and modelling of the thermodynamic properties of carbon dioxide mixtures with HFO-1234yf, HFC-125, HFC-134a, and HFC-32: vapour-liquid equilibrium, density, and heat capacity. *International Journal of Refrigeration* **2020**.
4. Akhfash, M.; Al Ghafri, S. Z.; Rowland, D.; Hughes, T. J.; Tsuji, T.; Tanaka, Y.; Seiki, Y.; May, E. F., Liquid and vapor viscosities of binary refrigerant mixtures containing R1234yf or R1234ze (E). *Journal of Chemical & Engineering Data* **2019,** *64* (3), 1122-1130.
5. Al Ghafri, S. Z.; Rowland, D.; Akhfash, M.; Arami-Niya, A.; Khamphasith, M.; Xiao, X.; Tsuji, T.; Tanaka, Y.; Seiki, Y.; May, E. F., Thermodynamic properties of hydrofluoroolefin (R1234yf and R1234ze (E)) refrigerant mixtures: Density, vapour-liquid equilibrium, and heat capacity data and modelling. *International Journal of Refrigeration* **2019,** *98*, 249-260.
6. Mylona, S. K.; Hughes, T. J.; Saeed, A. A.; Rowland, D.; Park, J.; Tsuji, T.; Tanaka, Y.; Seiki, Y.; May, E. F., Thermal Conductivity Data for Refrigerant Mixtures Containing R1234yf and R1234ze(E). *The Journal of Chemical Thermodynamics* **2019**.
7. Navarro-Esbrí, J.; Mendoza-Miranda, J. M.; Mota-Babiloni, A.; Barragán-Cervera, A.; Belman-Flores, J. M., Experimental analysis of R1234yf as a drop-in replacement for R134a in a vapor compression system. *International Journal of Refrigeration* **2013,** *36* (3), 870-880.
8. McLinden, M. O.; Kazakov, A. F.; Brown, J. S.; Domanski, P. A., A thermodynamic analysis of refrigerants: Possibilities and tradeoffs for Low-GWP refrigerants. *International Journal of Refrigeration* **2014,** *38*, 80-92.
9. Zilio, C.; Brown, J. S.; Schiochet, G.; Cavallini, A., The refrigerant R1234yf in air conditioning systems. *Energy* **2011,** *36* (10), 6110-6120.
10. Lemmon, E. W.; Bell, I. H.; Huber, M. L.; McLinden, M. O., NIST Standard Reference Database 23: Reference Fluid Thermodynamic and Transport Properties-REFPROP, Version 10.0, National Institute of Standards and Technology. 2018. *URL http://www. nist. gov/srd/nist23. cfm* **2018**.
11. Tanaka, Y.; Matsuo, S.; Taya, S., Gaseous thermal conductivity of difluoromethane (HFC-32), pentafluoroethane (HFC-125), and their mixtures. *International journal of thermophysics* **1995,** *16* (1), 121-131.
12. Ro, S. T.; Kim, M. S.; Jeong, S. U., Liquid thermal conductivity of binary mixtures of difluoromethane (R32) and pentafluoroethane (R125). *International journal of thermophysics* **1997,** *18* (4), 991-999.
13. Gao, X.; Assael, M. J.; Nagasaka, Y.; Nagashima, A., Prediction of the thermal conductivity and viscosity of binary and ternary HFC refrigerant mixtures. *International journal of thermophysics* **2000,** *21* (1), 23-34.
14. Tomimura, T.; Maki, S.; Zhang, X.; Fujii, M., Measurements of thermal conductivity and thermal diffusivity of alternative refrigerants in liquid phase with a transient short-hot-wire method. *Heat Transfer—Asian Research: Co-sponsored by the Society of Chemical Engineers of Japan and the Heat Transfer Division of ASME* **2004,** *33* (8), 540-552.

15. Ro, S. T.; Kim, J. Y.; Kim, D. S., Thermal conductivity of R32 and its mixture with R134a. *International journal of thermophysics* **1995,** *16* (5), 1193-1201.
16. Perkins, R. A.; Schwarzberg, E.; Gao, X. P. *Experimental thermal conductivity values for mixtures of R32, R125, R134a, and propane*; 1999.
17. Jeong, S. U.; Kim, M. S.; Ro, S. T., Liquid thermal conductivity of binary mixtures of pentafluoroethane (R125) and 1, 1, 1, 2-tetrafluoroethane (R134a). *International journal of thermophysics* **1999,** *20* (1), 55-62.
18. Assael, M. J.; Antoniadis, K. D.; Wakeham, W. A., Historical evolution of the transient hot-wire technique. *International journal of thermophysics* **2010,** *31* (6), 1051-1072.
19. Perkins, R. A.; Huber, M. L.; Assael, M. J., Measurements of the thermal conductivity of 1, 1, 1, 3, 3-Pentafluoropropane (R245fa) and correlations for the viscosity and thermal conductivity surfaces. *J. Chem. Eng. Data* **2016,** *61* (9), 3286-3294.
20. Assael, M. J.; Nieto de Castro, C. A.; Roder, H. M.; Wakeham, W. A., Transient methods for thermal conductivity. *Experimental Thermodynamics* **1991,** *3*, 161-195.
21. Perkins, R. A.; Roder, H. M.; Nieto de Castro, C. A., A high-temperature transient hot-wire thermal conductivity apparatus for fluids. *Journal of research of the National Institute of Standards and Technology* **1991,** *96* (3), 247-269.
22. Mylona, S. K.; Yang, X.; Hughes, T. J.; White, A. C.; McElroy, L.; Kim, D.; Al Ghafri, S.; Stanwix, P. L.; Sohn, Y. H.; Seo, Y.; May, E. F., High-Pressure Thermal Conductivity Measurements of a (Methane + Propane) Mixture with a Transient Hot-Wire Apparatus. *Journal of Chemical & Engineering Data* **2020,** *65* (2), 906-915.
23. Healy, J. J.; de Groot, J. J.; Kestin, J., The theory of the transient hot-wire method for measuring thermal conductivity. *Physica B+C* **1976,** *82*, 392-408.
24. Assael, M. J., Dix, M., Lucas, A., Wakeham, W. A., Absolute Determination of the Thermal Conductivity of the Noble Gases and Two of their Binary Mixtures as a Function of Density. *Journal Of The Chemical Society, Faraday Transactions 1* **1981,** *77*, 439-464.
25. Yang, X.; Arami-Niya, A.; Xiao, X.; Kim, D.; Ghafri, S. A.; Tsuji, T.; Tanaka, Y.; Seiki, Y.; May, E. F., Viscosity measurements of binary and multi-component refrigerant mixtures containing HFC-32, HFC-125, HFC-134a, HFO-1234yf and CO_2. *Journal of chemical & engineering data* **2020**.
26. ISO, I.; OIML, B., Guide to the Expression of Uncertainty in Measurement. *Geneva, Switzerland* **1995**.
27. Frenkel, M.; Chirico, R. D.; Diky, V.; Yan, X.; Dong, Q.; Muzny, C., ThermoData Engine (TDE): software implementation of the dynamic data evaluation concept. *J. Chem. Inf. Model.* **2005,** *45* (4), 816-838.
28. McLinden, M. O.; Klein, S. A.; Perkins, R. A., An extended corresponding states model for the thermal conductivity of refrigerants and refrigerant mixtures. *International Journal of Refrigeration* **2000,** *23* (1), 43-63.
29. Wuebbles, D. J., The role of refrigerants in climate change. *International journal of refrigeration* **1994,** *17* (1), 7-17.
30. Chichester, J. C.; Huber, M. L., Documentation and Assessment of the Transport Property Model for Mixtures Implemented in NIST REFPROP (Version 8.0). *National Institute of Standards and Technology* **2008**.
31. Ely, J. F.; Hanley, H., Prediction of transport properties. 2. Thermal conductivity of pure fluids and mixtures. *Industrial & Engineering Chemistry Fundamentals* **1983,** *22* (1), 90-97.
32. Ely, J. F.; Hanley, H., Prediction of transport properties. 1. Viscosity of fluids and mixtures. *Industrial & Engineering Chemistry Fundamentals* **1981,** *20* (4), 323-332.

Graphical abstract

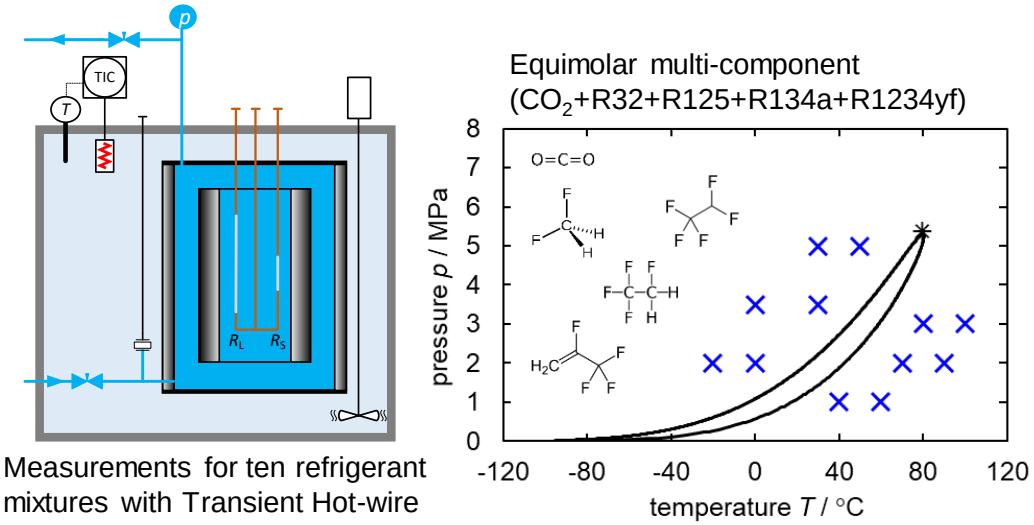

Measurements for ten refrigerant mixtures with Transient Hot-wire